LARGE LANDSLIDES IN LUNAR AND MERCURIAN IMPACT CRATERS. M. T. Brunetti[1], Z. Xiao[2,3], G. Komatsu[4], S. Peruccacci[1], and F. Guzzetti[1], [1]Research Institute for Geo-Hydrological Protection – Italian National Research Council (Via della Madonna Alta 126, 06128 Perugia, Italy, Maria.Teresa.Brunetti@irpi.cnr.it), [2]Planetary Science Institute, China University of Geosciences (430074, Wuhan, Hubei, P. R. China), [3]Centre for Earth Evolution and Dynamic, University of Oslo (Sem Selands vei 24, 0316 Oslo, Norway), [4]International Research School of Planetary Sciences, Università d'Annunzio (Viale Pindaro 42, 65127 Pescara, Italy)

Introduction: Landslides are one of the most significant geological processes shaping the surface of the Earth, and surface gravity is the main factor driving terrestrial mass movements. The effect of gravity can be investigated by comparing the size and morphology of mass failures in different Solar System bodies. To date, landslides have been observed on the Moon [1-3], Mars, e.g. [4-6], Venus [7], Mercury [8,9], and some icy satellites in the outer Solar System, e.g. [10]. Recent planetary exploration programs delivered a large volume of high-resolution imagery, which allows us to resolve and identify morphologic structures on planetary surfaces in detail. On Mars, large landslides detected in Valles Marineris are hypothesized to be seismically induced [6,11]. Numerous landslides of various scales have been observed on the Moon, from mass movements less than 1 km^2 in area [3] to larger landslides on the ejecta deposit of the Tsiolkovskiy basin [12]. On Mercury, formerly studied landslides are large-scale failures associated with crater ejecta deposits and they are somewhat similar to layered ejecta deposits on Mars [8]. Here, we focus on large slope failures observed on internal walls of impact craters on the Moon and Mercury.

Methodology: To recognize and map the landslides on the two planetary bodies, we adopted the same visual criteria (e.g., color, tone, pattern, and texture of images) commonly used by geomorphologists to identify landslides in aerial photographs or satellite images on the Earth (e.g. [13]).

For the Moon, we visually analyzed images acquired at 100 m/pixel resolution by the Wide Angle Camera onboard the Lunar Reconnaissance Orbiter Camera [14]. For Mercury, we examined images at an average resolution of 250 m/pixel obtained by the Wide Angle Camera onboard the MESSENGER spacecraft [15].

In order to analyze the effect of the surface gravity in the slope failure mechanism, we focused on probable post-impact landslide features, as opposed to terraces formed during the modification stage of impact cratering.

We selected and mapped large landslides in cavities that do not exhibit an inward collapse involving the full crater rim. The aim is to deal with mass movements driven by the planet surface gravity, and not induced by the energy released during the impact process itself. It is believed that the trigger of post-impact landslides is seismic shaking caused by nearby impacts [16].

Figure 1 shows two examples of craters hosting landslides on the Moon (a) and Mercury (c), respectively, and the corresponding failures (b) and (d) mapped in the two cavities. To better identify the landslide scarp that deformed the crater rim, we traced a circle that likely represents the early transient crater (blue circles in Figure 1b and 1d). We mapped separately the scarp (purple and red shaded areas) and the deposit (green and light blue shaded areas).

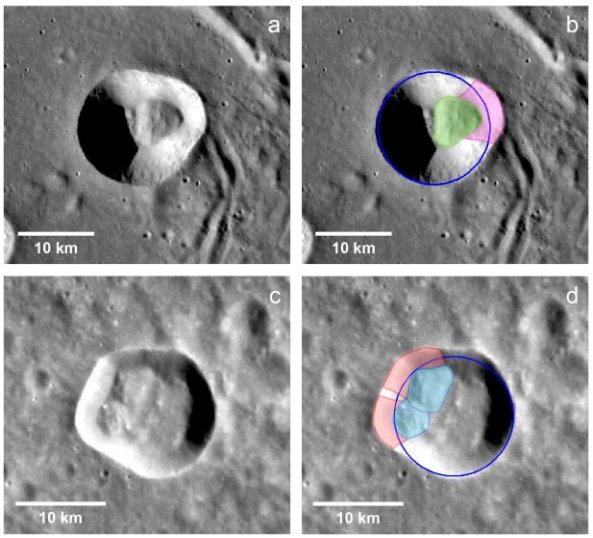

Figure 1. Example of craters hosting landslides on the Moon (a) and Mercury (c) and the mapped mass movements (b) and (c). Landslide scarps are the purple and red shaded areas; deposits are the green and light blue shaded areas.

Results: We compiled two new inventories of (i) 60 landslides mapped in 35 craters on the Moon and (ii) 58 landslides mapped in 38 craters on Mercury. Adopting categories used to catalogue terrestrial mass movements, landslides in the two inventories were classified as rock slides. We obtained the planimetric area, A_L, of the mapped failures in a GIS, and we calculated the probability density distribution of the landslide area for the Moon and Mercury (grey and orange dots in Figure 2).

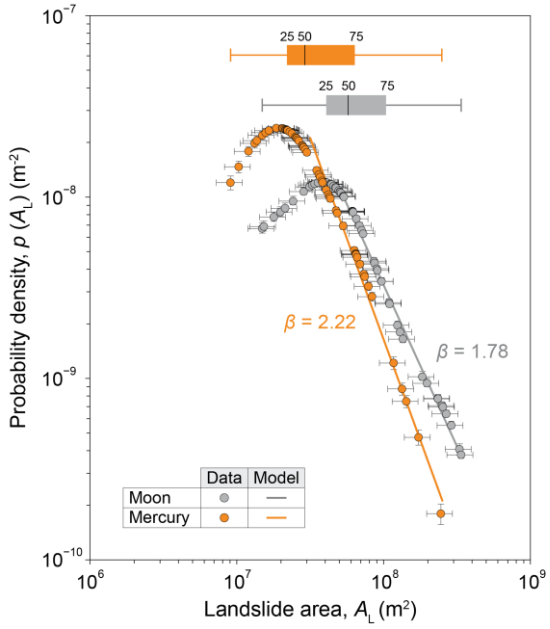

Figure 2. Probability distributions of landslide area on the Moon and Mercury. $p(A_L)$ is the non-cumulative probability density of landslide area for 60 rock slides mapped on the Moon (purple) and 58 rock slides on Mercury (orange). Colour lines show corresponding best fit models of the distribution tails. Box plots show statistics of A_L for both data sets.

Inspection of Figure 2 reveals that rock slides mapped in impact craters on the Moon are on average larger than analogous rock slides on Mercury, which begin to occur at smaller scales. The two distributions exhibit different modal values, the mode of Mercury being lower (A_L = $2 \cdot 10^7$ m^2) than that of the Moon (A_L = $4 \cdot 10^7$ m^2). This result could be an effect of the stronger surface gravity of Mercury (3.70 m·s^{-1}) compared to the Moon (1.60 m·s^{-1}). For landslides larger than about $4 \cdot 10^7$ m^2, the probability is always smaller on Mercury than on the Moon, indicating that more larger landslides are likely to occur on the Moon. This could be a consequence of a lower mobility of landslide materials on Mercury.

The scaling exponent, β, calculated for Mercury is higher than that obtained for the Moon and is similar to what is found for the terrestrial landslides, where β = 2.2 to 2.4 [17].

We also investigated the relationship between the individual rock slide area, A_L, and the area of the early transient crater, A_C, and we compared the results from the two inventories (Figure 3). We found that rock slides on Mercury initiate at a smaller crater area. The above finding seems to confirm the effect of the weaker surface gravity of the Moon compared to that of Mercury.

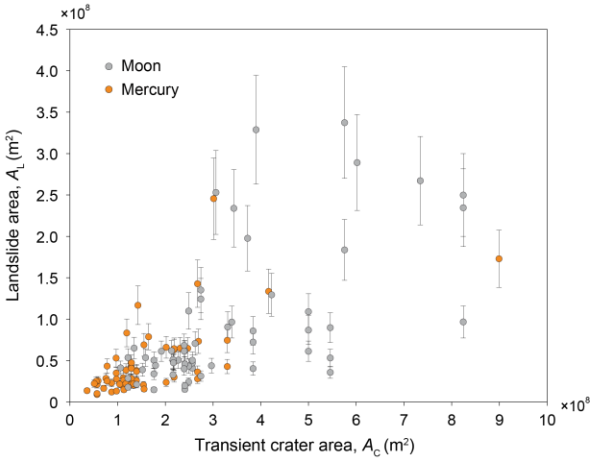

Figure 3. Probability distributions of landslide area, A_L, on the Moon (grey dots) and on Mercury (orange dots) as a function of the early transient crater area, A_C.

The largest landslides are in the range of complex craters for the Moon and Mercury [18]. These landslides are possibly incomplete terracing during the modification stage of the crater, which can have experienced different conditions for downward movement of inner rim materials from typical landslides.

References: [1] Pike R. J. (1971) *NASA SP-232*, 14–20. [2] Lindsay J. (1976) In (Kopal Z., Cameron A. G. W., eds) *Developments in Solar System and Space Science, Vol. 3*, 45–55. [3] Xiao Z. et al. (2013) *Earth Planet. Sci. Lett. 376*, 1–11. [4] McEwen A.S. (1989) *Geology, 17*, 1111–1114. [5] Shaller P. J., and Komatsu G. (1994) *Landslide News 8*, 18–22. [6] Brunetti M. T., e al. (2014) *Earth Planet. Sci. Lett. 405*, 156–168. [7] Malin M. C. (1992) *J. Geophys. Res. Planets 97*, 16337–16352. [8] Xiao Z. and Komatsu G. (2013) *Planet. Space Sci. 82-83*, 62–78. [9] Blewett D. T. et al. (2013) *J. Geophys. Res. Planets 118*, 1013–1032. [10] Schenk P. M. and Bulmer M. K. (1998) *Science 279*, 1514–1517. [11] Crosta G. B. et al. (2014) *Earth Planet. Sci. Lett. 388*, 329–342. [12] Melosh, H. J. (1989). *Oxford University Press*, New York, pp. 245. [13] Guzzetti F. et al. (2012) *Earth Sci. Rev. 112(1-2)*, 42–66. [14] Robinson M. S. et al. (2010) *Space Sci. Rev. 150(1-4)*, 81–124. [15] Hawkins, S. E. III et al. (2007) *Space Sci. Rev. 131*, 247–338. [16] Wood C. A. (2012) *43rd LPSC*, Abstract #1637. [17] Malamud B. D. (2004) *Earth Surf. Proc. Land. 29(6)*, 687–711. [18] Pike R. J. (1980) *11th LPSC*, Abstract 700–702.